5

SOFT SPHERES

As illustrated in Figure 5.1, dynamic modeling divides into two tasks: developing a model and using the model in a simulation. The first task, model development, includes choosing a form for the intermolecular potential and then deriving appropriate equations of motion. In this chapter we tackle simulation of substances modeled as soft spheres, substances for which the prototypical potential is that proposed by Lennard-Jones. In Section 5.1 we describe the Lennard-Jones model, how it is often modified for use in molecular dynamics, and how those modifications help simplify the simulation.

After we have chosen the model potential, we must formulate equations of motion. Since in this book we consider only isolated systems, the equations of motion are simply obtained from Newton's second law. Those equations are discussed in Chapter 2 and methods for solving them are described in Chapter 4, so equations of motion are ignored here.

Again as in Figure 5.1, the second modeling task—the simulation—itself divides into two parts: generating phase-space trajectories and analyzing the trajectories for properties. Trajectory generation claims most of our attention in this chapter; in particular, trajectory generation decomposes into initialization (Section 5.2), equilibration (Section 5.3), and production (Section 5.4). Trajectory analysis is discussed in detail in Chapters 6 and 7; however, some analysis must be done during each run to check that the run is proceeding correctly, to identify the onset of equilibrium, and to help decide when the run can be stopped. This ongoing analysis is described in Section 5.5. Although trajectory generation is discussed here in terms of the Lennard-Jones model, in fact, the discussions in this chapter generally apply to any continuous pair potential acting between spherical objects.
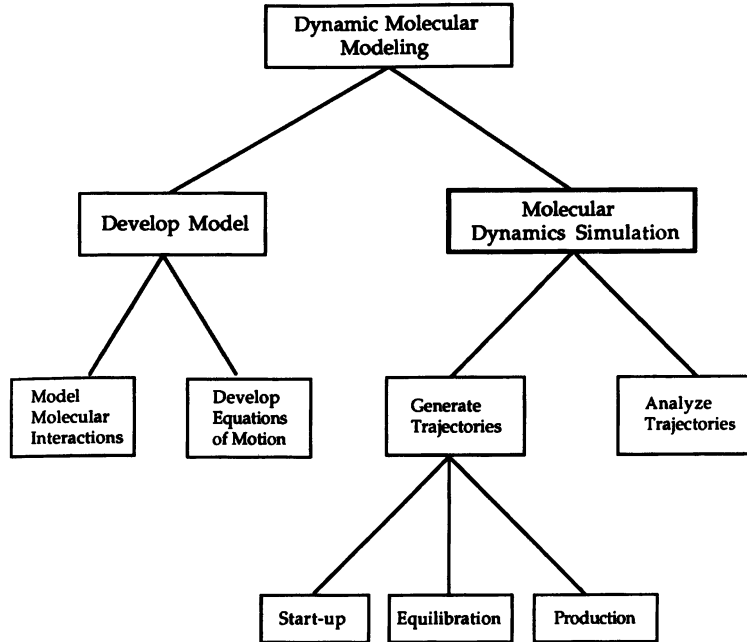
188

FIGURE 5.1   Steps in dynamic modeling of matter.

5.1   INTERMOLECULAR POTENTIAL MODELS

As the first step in performing a simulation we must choose a functional form for the intermolecular potential $\mathcal{U}(\mathbf{r}^N)$. Nearly always, we take the potential to be pairwise additive; that is, we assume the interaction energy among N atoms is a sum of isolated two-body contributions. For spheres, the pairwise additive form is

$$\mathcal{U}(\mathbf{r}^N) = \sum_{i<j}\sum u(r_{ij}) \tag{5.1}$$

Recall $\mathbf{r}^N$ is a shorthand for the set of sphere position vectors (Figure 2.1), $\mathbf{r}^N = \{\mathbf{r}_1,\mathbf{r}_2,\mathbf{r}_3,\ldots,\mathbf{r}_N\}$, u is a two-body potential, and r_{ij} is the scalar distance between the centers of atoms i and j, $r_{ij} = |\mathbf{r}_i - \mathbf{r}_j|$. The form (5.1) neglects simultaneous multibody interactions which, if included, would drastically increase the time required for a simulation.

In 1924 J. E. Lennard-Jones introduced [1] a useful model for the soft-sphere pair potential

$$u(r) = k\varepsilon\left[\left(\frac{\sigma}{r}\right)^n - \left(\frac{\sigma}{r}\right)^m\right] \tag{5.2}$$

where

$$k = \frac{n}{n-m}\left(\frac{n}{m}\right)^{m/(n-m)}$$

(5.3)

Unlike the hard-sphere potential, the Lennard-Jones model attempts to account both for short-range, repulsive overlap forces and for longer range, attractive dispersion forces. Short-range repulsive forces prevent the substance from collapsing onto itself, while longer range attractions deter disintegration of the substance (in the absence of a container). These forces have range and strength determined by the values assigned to the integers n and m $(n > m)$. For m the common choice is $m = 6$, primarily because the leading term in London's theory [2] for dispersion varies as $1/r^6$. Popular wisdom then sets $n = 2m = 12$, which has the merit of a kind of logic while lacking any particular physical justification. The resulting Lennard-Jones (12,6) model is

$$u(r) = 4\varepsilon\left[\left(\frac{\sigma}{r}\right)^{12} - \left(\frac{\sigma}{r}\right)^{6}\right]$$

(5.4)

The remaining parameters in (5.4) are σ, the distance to the zero in $u(r)$, and ε, the energy at the minimum in $u(r)$; see Figure 5.2. Since intermolecular forces are necessarily conservative, the force that results from the potential (5.4) is

$$F(r) = -\frac{du(r)}{dr} = 24\frac{\varepsilon}{\sigma}\left[2\left(\frac{\sigma}{r}\right)^{13} - \left(\frac{\sigma}{r}\right)^{7}\right]$$

(5.5)

By convention, repulsive forces are positive while attractive forces are negative.

5.1.1 Truncated Potential

In a system of N atoms, the double sum in (5.1) accumulates $\frac{1}{2}N(N-1)$ unique pair interactions. Thus, if all pair interactions are sampled during a simulation, the number of such samples increases with the square of the number of atoms. Further, if the allowed range of interaction between atoms is increased, say from r to $r + \Delta r$, then the number of sampled interactions increases as r^2; that is,

$$N(r, \Delta r) \approx \rho V(r, \Delta r) \approx 4\pi\rho r^2 \Delta r$$

(5.6)

Here ρ is the number density, $N(r, \Delta r)$ is the number of atoms in a spherical shell of radius r and thickness Δr, and $V(r, \Delta r)$ is the volume of the shell.
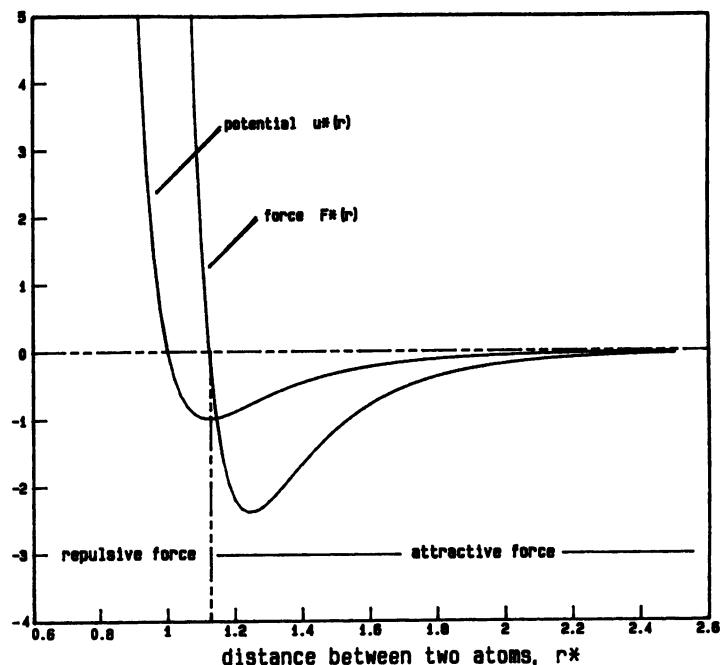
FIGURE 5.2 Lennard-Jones $(12,6)$ pair potential (5.4) and pair force (5.5). The units here are $r^* = r/\sigma$, $u^* = u/\varepsilon$, and $F^* = F\sigma/\varepsilon$.

From Figure 5.2 we see that the Lennard-Jones potential extends over a modest range of pair separations; as a result, we can achieve a considerable savings in computer time by neglecting pair interactions beyond some distance r_c. Therefore the Lennard-Jones potential actually used in simulations is a truncated version of (5.4),

$$u(r) = \begin{cases} 4\varepsilon\left[\left(\dfrac{\sigma}{r}\right)^{12} - \left(\dfrac{\sigma}{r}\right)^{6}\right] & r \leq r_c \\ 0 & r > r_c \end{cases} \qquad (5.7)$$

A common choice for r_c is 2.5σ, at which $u = -0.0163\varepsilon$ and the force $F = -0.039\varepsilon/\sigma$. Thus, when $r_{ij} = r_c$, atom j makes only a small contribution to the force on atom i.

Because of the truncation at r_c, a simulation can provide only a portion of those properties, such as the internal energy and pressure, that are directly related to the potential. Simulation results for such properties must be corrected for long-range interactions $(r > r_c)$ that are neglected during a run. To estimate these long-range corrections, formulas are given in Chapter 6.

Truncating the potential at r_c introduces a similar truncation into the force which, in turn, causes small impulses on atoms i and j whenever their separation distance r_{ij} crosses r_c. Consequently, instead of a strictly constant total energy E, we may observe small fluctuations in E. These fluctuations little affect values computed for equilibrium properties, and of course, the effects can be made negligible by simply increasing r_c at the expense of increased computer time for the simulation.

5.1.2   Shifted-Force Potential

When we test a simulation code, small fluctuations in the total energy can obscure small errors, frustrating the test. For testing purposes, the step change in $u(r)$ and $F(r)$ can be removed by shifting $F(r)$ vertically so that the force goes smoothly to zero at r_c. Hence, define a shifted force $F_s(r)$ by [3]

$$F_s(r) = \begin{cases} -\dfrac{du}{dr} + \Delta F & r \le r_c \\ 0 & r > r_c \end{cases} \tag{5.8}$$

where ΔF is the magnitude of the shift,

$$\Delta F = -F(r_c) = \left(\frac{du}{dr}\right)_{r_c} \tag{5.9}$$

The shifted-force potential $u_s(r)$ corresponding to $F_s(r)$ can be derived from

$$F_s(r) = -\frac{du_s(r)}{dr} \tag{5.10}$$

or

$$\int_0^{u_s} du_s = -\int_\infty^r F_s(r)\, dr \tag{5.11}$$

Substituting (5.8) into (5.11) and integrating gives

$$u_s(r) = \begin{cases} u(r) - u(r_c) - [r - r_c]\left(\dfrac{du}{dr}\right)_{r_c} & r \le r_c \\ 0 & r > r_c \end{cases} \tag{5.12}$$

Figure 5.3 compares this shifted-force potential with the full Lennard-Jones model.
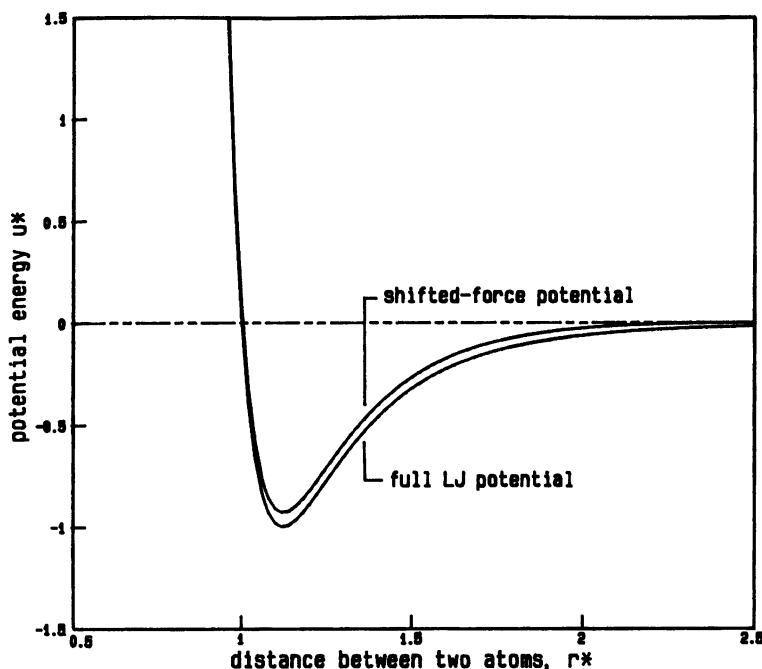
FIGURE 5.3 Comparison of the full Lennard-Jones (LJ) potential (5.4) and the shifted-force potential (5.12), with the shift applied at $r_c = 2.5\sigma$. Here $u^* = u/\varepsilon$ and $r^* = r/\sigma$.

Using (5.8) and (5.12) in place of (5.7) removes energy fluctuations that occur because of the truncation of u and F. However, if the shifted-force potential is used to evaluate properties, then corrections must be included to account for both the long-range interactions (as discussed in Section 5.1.1) and the shift [3]. The shifted-force corrections are approximate and cumbersome to compute, and so we recommend that the shifted-force model be used only as an aid in verifying codes: it should not be used to determine properties in production runs.

5.1.3 Minimum-Image Criterion

In a system whose N atoms interact via a pairwise additive potential, the force vector exerted by atom j on atom i is given, at any instant, by

$$\mathbf{F}_i = -\frac{\partial u(\mathbf{r}_{ij})}{\partial \mathbf{r}_i} \tag{5.13}$$

However, in periodic systems forces can be exerted by image atoms, as well

as by real atoms (Section 2.9), and so (5.13) is replaced by

$$\mathbf{F}_i = -\sum_\alpha \frac{\partial u(\mathbf{r}_{ij} - \alpha L)}{\partial \mathbf{r}_i} \tag{5.14}$$

Here $\mathbf{r}_{ij} - \alpha L = \mathbf{r}_i - (\mathbf{r}_j + \alpha L)$, L is the length of one edge of the primary cell, and α is the cell translation vector discussed in Section 2.9. In a D-dimensional system the sum over α in (5.14) is a D-fold sum, as in (2.106).

When the forces are short ranged compared to L, we need consider only those image cells that adjoin the primary cell. Then in three dimensions (5.14) becomes

$$\mathbf{F}_i = -\sum_{\alpha_x = -1}^{+1} \sum_{\alpha_y = -1}^{+1} \sum_{\alpha_z = -1}^{+1} \frac{\partial u(\mathbf{r}_{ij} - \alpha L)}{\partial \mathbf{r}_i} \tag{5.15}$$

The triple sum in (5.15) accumulates forces from atom j and each of its 26 images; however, of the 27 terms in (5.15), only one has a separation $|\mathbf{r}_{ij} - \alpha L|$ less than $\frac{1}{2}L$. Therefore, if the pair potential $u(r_{ij})$ is truncated at $r_c \le \frac{1}{2}L$, then either atom j or, at most, only *one* of its images can exert a force on atom i. The interaction distance is necessarily the smallest of the 27 possibilities: this identifies the *minimum image criterion* for computing forces. Thus, in periodic systems, when the interaction is truncated at $r_c \le \frac{1}{2}L$, the minimum image criterion selects from the triple sum in (5.15) the one nonzero term—that for the smallest of the 27 distances $\{|\mathbf{r}_{ij} - \alpha L|, (\alpha_x = -1, 1), (\alpha_y = -1, 1), (\alpha_z = -1, 1)\}$.
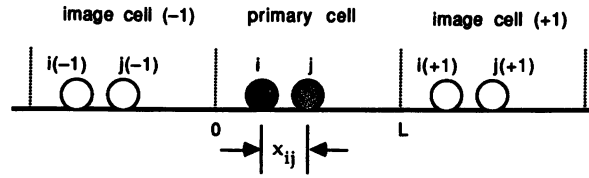
To develop a procedure for finding the minimum image distance, we can consider a one-dimensional system with periodic boundaries, as in Figure 5.4. In the figure the primary "cell" has width L and contains two particles, $i(0)$ and $j(0)$. Because the system is one dimensional, the primary cell has only two adjacent image cells, one identified by $\alpha_x = +1$, the other by $\alpha_x = -1$. In one dimension the force, analogous to (5.15), is

$$F_i = -\sum_{\alpha_x = -1}^{+1} \frac{\partial u(x_{ij} - \alpha_x L)}{\partial x_i} \tag{5.16}$$
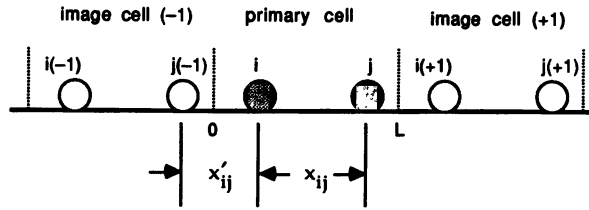
To obtain the force, we must consider the three values of α_x, any one of which might give the smallest distance $|x_{ij} - \alpha_x L|$:

Situation A in the figure ($\alpha_x = 0$) has $x_{ij} < \frac{1}{2}L$. In this case the distances between i and either j image are greater than $\frac{1}{2}L$ and hence greater than r_c. The images do not interact with i, and therefore the

Situation A: $x_{ij} < L/2$

image cell (-1)   primary cell   image cell (+1)

| i(-1) j(-1) | | i   j | | i(+1) j(+1) |

0 — x_{ij} — L

Situation B: $x_{ij} < -L/2$ $x_{ij} \rightarrow x'_{ij} = x_{ij} + L$

image cell (-1)   primary cell   image cell (+1)

| i(-1)   j(-1) | | i   j | i(+1)   j(+1) |

0   L

x'_{ij} x_{ij}

Situation C: $x_{ij} > L/2$ $x_{ij} \rightarrow x'_{ij} = x_{ij} - L$

image cell (-1)   primary cell   image cell (+1)

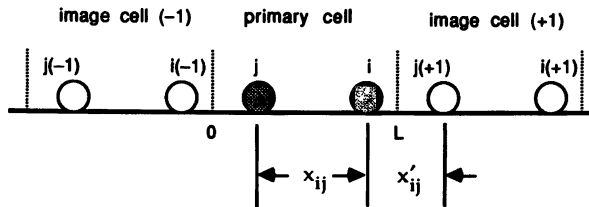| j(-1)   i(-1) | | j   i | j(+1)   i(+1) |

0   L

x_{ij} x'_{ij}

FIGURE 5.4 Three possible situations that can occur when applying the minimum image criterion for determining force between atoms i and j in a one-dimensional periodic system.

distance between i and j in the primary cell is the appropriate distance to use in (5.16) for evaluating the force.

Situation B in Figure 5.4 ($\alpha_x = -1$) has $x_{ij} < -\frac{1}{2}L$. In this case $|x_{ij}| > r_c$ and j does not interact with i via the truncated potential. However, the image $j(-1)$ is within r_c of i and does interact; so the distance x_{ij} becomes

$$x_{ij} \rightarrow x_i - x_{j(-1)} = x_i - \left[x_{j(0)} - L \right] = x_{ij} + L \qquad (5.17)$$

The other image, $j(+1)$ lies more than $\frac{1}{2}L$ from i and therefore does not interact.

Situation C in Figure 5.4 ($\alpha_x = +1$) has $x_{ij} > \frac{1}{2}L$. In this case $x_{ij} > r_c$ and j does not interact with i. However, the image $j(+1)$ is within r_c of i and does interact; so

$$x_{ij} \to x_i - x_{j(+1)} = x_i - \left[x_{j(0)} + L\right] = x_{ij} - L \qquad (5.18)$$

For a cubic container in three dimensions, the minimum image criterion applies separately to each Cartesian component of the pair separation vector $\mathbf{r}_{ij}$; thus, for the x component, we use $x_{ij} \to x_{ij} - \alpha_x L$ where $\alpha_x = 0$ if $-\frac{1}{2}L \le x_{ij} \le \frac{1}{2}L$, $\alpha_x = -1$ if $x_{ij} < -\frac{1}{2}L$, and $\alpha_x = +1$ if $x_{ij} > \frac{1}{2}L$. Similarly for y_{ij} and z_{ij}.

5.1.4 Neighbor Lists

The most time-consuming part of a molecular dynamics simulation is calculation of the forces on the atoms. For a fluid of N atoms, the forces are computed by sampling, at each time step of the simulation, $\frac{1}{2}N(N-1)$ unique r_{ij} distances. But when a truncated potential is used, the force equals zero for any $r_{ij} > r_c$ (where r_c is the potential cutoff distance described in Section 5.1.1); consequently, evaluating distances r_{ij} that are greater than r_c wastes computer time.

This wasted time can be saved by using a bookkeeping scheme such as that originally devised by Verlet [4]. For each atom i, the method maintains a list of neighboring atoms that lie within a distance r_L of i; so the list identities those atoms that contribute to the force on atom i. The same neighbor list is used over several consecutive time steps, and it is updated periodically, say every 10 time steps. The list distance r_L is slightly larger than r_c so that j atoms can cross r_c and still be properly considered in evaluating the force on i. Typically, $r_L = r_c + 0.3\sigma$.

For a three-dimensional Lennard-Jones fluid at density $\rho\sigma^3 = 0.8$, each atom has about 75 neighbors lying within a radius $r = 2.8\sigma$ (which is the appropriate list distance when $r_c = 2.5\sigma$). However, in the neighbor list for atom i, we need store only the identities of those neighbors j having $j > i$, because for $j < i$ atom i appears in the list as a neighbor of j. On average, about half the neighbors of i have $j > i$, so we need, for the neighbor list, about $\frac{75}{2} \approx 40$ storage locations per atom. Therefore to store the neighbor list in a simulation of 256 atoms, we use an array, call it LIST, containing about 11,000 elements. We then use the elements of another array, NPOINT, to locate in LIST the neighbors of a particular atom. The relation between NPOINT and LIST is illustrated in Figure 5.5. By using two one-dimensional arrays rather than one two-dimensional array, we avoid the computational
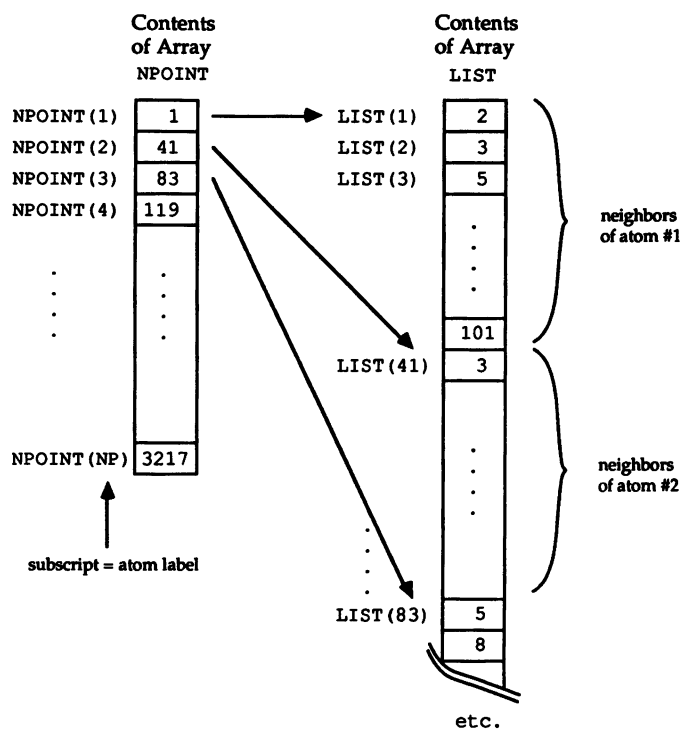
FIGURE 5.5 Use of two one-dimensional arrays to store a neighbor list for each atom during a simulation of a system containing N atoms.

overhead involved in dealing with double subscripted variables. A neighbor list can provide substantial gains in execution speed, as shown in Table 5.1.

The scheme just described is but one way by which a neighbor list can be implemented. It has the disadvantage that it does not vectorize to run on parallel machines; however, modifications can be made to overcome this handicap [5-9].

TABLE 5.1   Speed of Execution of Lennard-Jones Program with and without a Neighbor List, $\langle kT/\varepsilon \rangle = 1.095$

$\rho\sigma^3$	N	Average Number of Neighbors Stored per Atom	Relative Number of Time Steps Executed	
			No List	With List[a]
0.6	108	27.2	6.7	9.7
	256	27.5	1	3.3
0.85	108	28.0	5.3	8.1
	256	38.1	1	2.6

[a] $r_c = 2.5\sigma$, $r_L = 2.8\sigma$, list up-dated every 10 time-steps.

5.2 INITIALIZATION

With a form chosen for the model potential, we can turn to the use of the model in a molecular dynamics simulation. For the chosen model, a simulation generates a portion of the phase-space trajectory, and as shown in Figure 5.6, trajectory generation involves initialization, equilibration, and production. In this section we consider initialization, which we divide into two parts: decisions concerning preliminaries and initialization of the atoms. The preliminaries include a system of units in which the calculation will be carried out, the finite-difference algorithm to be used, and assignment of values to parameters that remain constant during a run. The preliminaries are discussed in Section 5.2.1. Initialization of the atoms means assignment of initial positions, initial velocities, and (perhaps) initial values for higher derivatives of the positions. These assignments are discussed in Section 5.2.2.

5.2.1 Preliminaries

System of Units. Simulation programs are conventionally written so that all quantities are unitless. As units of distance and energy we use the potential parameters σ and ε, respectively, and as the unit of mass, that of one atom.
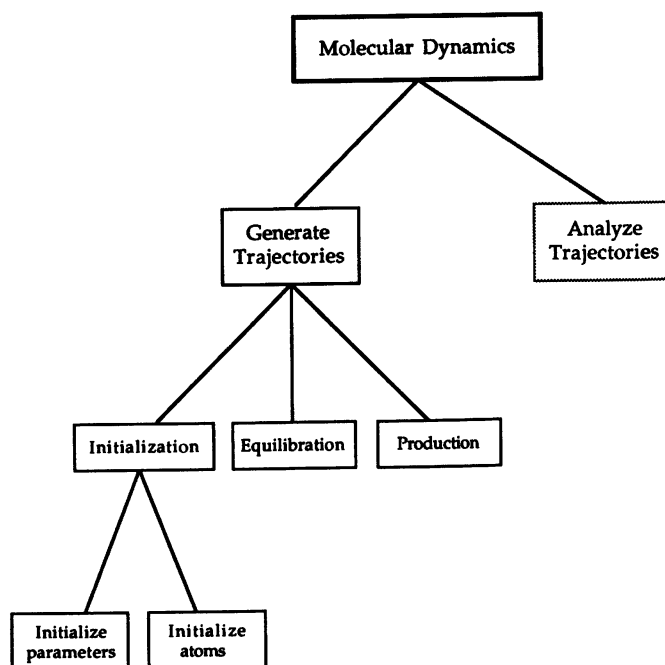

FIGURE 5.6 Trajectory generation divides into initialization, equilibration, and production.

TABLE 5.2 System of Units[a] Used in Soft-Sphere Molecular Dynamics Programs

Fundamental Quantities

Mass m = mass of one atom
Length σ
Energy ε
Time $\sigma\sqrt{m/\varepsilon}$

Derived Quantities

Adiabatic compressibility	$\kappa_s^* = \kappa_s \varepsilon / \sigma^3$
Configurational internal energy	$U_c^* = U_c / N\varepsilon = \langle \mathscr{U}^* \rangle = \langle \mathscr{U}/N\varepsilon \rangle$
Density	$\rho^* = N\sigma^3 / V$
Force	$F^* = F\sigma / \varepsilon$
Heat capacity	$C_v^* = C_v / Nk$
Radial position	$r^* = r / \sigma$
Pressure	$P^* = P\sigma^3 / \varepsilon$
Temperature	$T^* = kT / \varepsilon$
Thermal pressure coefficient	$\gamma_v^* = \gamma_v \sigma^3 / k$
Total energy	$E^* = E / N\varepsilon$
Velocity	$v^* = v\sqrt{m/\varepsilon}$

[a]W. Thomson, Lecture XVI, p. 158: "The distinguishing feature of an engineer is the quickness with which he can reduce from square feet to acres, and so on. If his brain were free from that, he might do more elsewhere, and have more time to find out about the properties of matter."

The unitless (or reduced) forms for quantities are indicated by an asterisk; for example, (5.4) for the Lennard-Jones potential becomes

$$u^*(r^*) = 4\left[\left(\frac{1}{r^*}\right)^{12} - \left(\frac{1}{r^*}\right)^6\right] \tag{5.19}$$

where $u^* = u/\varepsilon$ and $r^* = r/\sigma$. The reduced forms for other derived quantities are given in Table 5.2.

State Condition. For equilibrium molecular dynamics performed on isolated systems, the independent thermodynamic properties are the number of molecules N, system volume V, and total energy E. Then for a one-phase system, specifying values for the number density $\rho^* = N\sigma^3/V$ and the energy per atom $E^* = E/N\varepsilon$ determines the thermodynamic state. Usually, $100 < N < 1000$, with the particular value of N taken to be large enough to properly capture the phenomena of interest yet small enough to prevent the simulation from being prohibitively expensive. Having picked N, the required value of V is obtained from the assigned density ρ^*.

Assigning a value to E^* may be accomplished by scaling the atomic velocities. Let subscripts D and A designate "desired" and "actual" values for properties. For example, based on the initially assigned atomic positions and velocities, the actual total energy is

$$E_A^* = E_{kA}^* + \mathscr{U}^* \tag{5.20}$$

Using the desired set point for the total energy E_D^* and the computed potential energy $\mathscr{U}^*$, we can compute a required value for the kinetic energy

$$E_{kD}^* = E_D^* - \mathscr{U}^* \tag{5.21}$$

Then we scale each initially assigned component of a velocity vector according to

$$v_{ix}^{*\,new} = v_{ix}^* \sqrt{\frac{E_{kD}^*}{E_{kA}^*}} = v_{ix}^* \sqrt{\frac{E_D^* - \mathscr{U}^*}{E_A^* - \mathscr{U}^*}} \tag{5.22}$$

The same scaling is also applied to the y- and z-components. By substituting these new velocities into

$$E^* = \frac{1}{2N} \sum_i \mathbf{v}_i^* \cdot \mathbf{v}_i^* + \mathscr{U}^*(r^N) \tag{5.23}$$

we can verify that the set-point energy E_D^* is indeed obtained. Here, as in all that follows, we follow the convention in Table 5.2 that sets the atomic mass to unity.

Usually, instead of density and energy (ρ^*, E^*), we would like to establish the thermodynamic state using density and temperature (ρ^*, T^*). This may be achieved by scaling the initially assigned velocities to obtain a desired kinetic energy rather than a desired total energy. The procedure takes advantage of the relation (2.43) between absolute temperature and time-average kinetic energy,

$$T^* = \frac{1}{3N} \left\langle \sum_i \mathbf{v}_i^* \cdot \mathbf{v}_i^* \right\rangle \tag{5.24}$$

Thus, rather than apply the scaling (5.22), we scale the initial velocities $\mathbf{v}_i(0)$ so that initially we have the desired temperature T_D^*

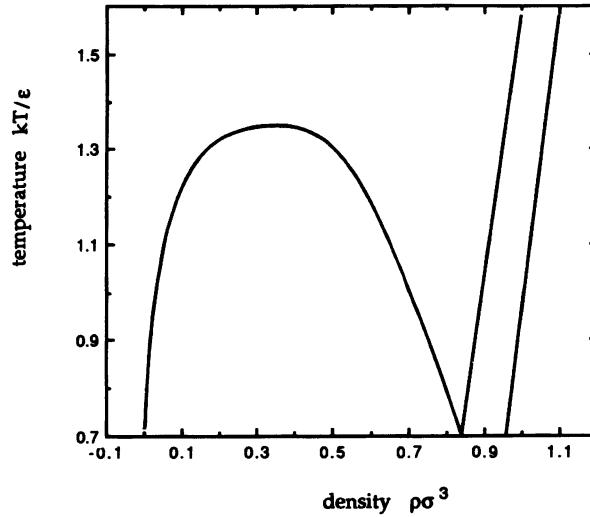$$v_{ix}^{*\,new} = v_{ix}^* \sqrt{\frac{T_D^*}{T_A^*}} \tag{5.25}$$

FIGURE 5.7 Temperature–density phase diagram for the pure Lennard-Jones $(12,6)$ substance. The vapor–liquid saturation curve was computed using the Nicolas et al. [3] equation of state. The melting lines were taken from Hansen and McDonald [10].

where T_A^* is the actual temperature computed from (5.24) using the initially assigned velocities. A similar scaling is applied to the y- and z-components of $v_i^*(0)$.

Because kinetic energy is not a constant of the motion, the scaling (5.25) is less effective in achieving a set-point temperature than is the scaling (5.22) in achieving a set-point energy. During the initial phase of a run, as the system relaxes from its initial condition, energy will be exchanged between the potential and kinetic modes; consequently, the temperature will drift from its set point. To compensate, the scaling (5.25) is normally continued over the full equilibration phase. After scaling for a few hundred time-steps, the state condition will be close but not exactly equal to the desired one. To facilitate the choice of state conditions, we give in Figure 5.7 the temperature–density phase diagram for the pure Lennard-Jones $(12,6)$ substance.

Boundary Conditions, Algorithm, and Time-Step. For simulations of bulk fluids, unwanted surface effects are removed by using periodic boundary conditions (pbc). Periodic boundary conditions are discussed in Section 2.9, and so here we merely note that to apply pbc, the volume holding the atoms must be space filling. In three dimensions the simplest space-filling shape is the cube: the cube provides the simplest pbc transformations (2.114). Therefore most bulk substance simulations are done on cubic containers, with the length L^*

of one edge of the cube determined from the assigned density ρ^*

$$L^* = \frac{L}{\sigma} = \left(\frac{N}{\rho^*}\right)^{1/3} \tag{5.26}$$

With the potential model, state condition, and container geometry chosen, we must now select an algorithm for solving the equations of motion. To have a concrete example, we choose the Gear predictor–corrector method discussed in Section 4.4.3. To apply the algorithm, we need a value for the integration time-step Δt. The optimum value of Δt is a compromise. It should be large to sample as much of phase space as possible; however, it should be small compared to the mean time between molecular collisions, for otherwise the algorithm will be unstable. For the Lennard-Jones fluid, an acceptable value is $\Delta t^* = 0.005$. Using $\varepsilon/k = 120$ K, $\sigma = 3.405$ Å, and the argon value for atomic mass, $\Delta t^* = 0.005$ corresponds to $\Delta t \approx 10^{-14}$ sec. With this tentative value for Δt, test runs can be done to study how the code performs with changes in time-step.

5.2.2 Initial Conditions for Atoms

To start the finite-difference algorithm, atomic positions r_i and their time derivatives must be assigned at time $t = 0$. The positions r_i are measured with respect to some space-fixed frame, such as in Figure 5.8, and their initial values $r_i(0)$ may be assigned according to some lattice structure or taken from a previous simulation. They should not be assigned randomly because random assignments often create artificially large overlaps of adjacent atoms; such overlaps produce an unphysically large repulsive force that can cause numerical failure of the finite-difference algorithm. When positions are assigned to a lattice, a face-centered-cubic (fcc) structure is usually used because argon crystallizes into an fcc structure. The construction of an fcc lattice is discussed in Section 3.4 and need not be repeated here.

Initial velocities $v_i(0)$ may be randomly assigned or they may be taken from a previous simulation. For randomly assigned velocities let ξ_x, ξ_y, and ξ_z represent three random numbers each uniformly distributed over the interval $[-1, +1]$. Then the Cartesian components of $v_i(0)$ are assigned by

$$v_{ix}^*(0) = \frac{\xi_x}{\xi} \qquad v_{iy}^*(0) = \frac{\xi_y}{\xi} \qquad v_{iz}^*(0) = \frac{\xi_z}{\xi} \tag{5.27}$$

where $\xi \equiv \sqrt{\xi_x^2 + \xi_y^2 + \xi_z^2}$. These initial velocities are scaled either according to (5.22) to produce the set-point total energy or according to (5.25) to produce the set-point temperature.

Since no external forces act on the system, the total linear momentum should be conserved (Section 2.10). Moreover, the substance is static; there-
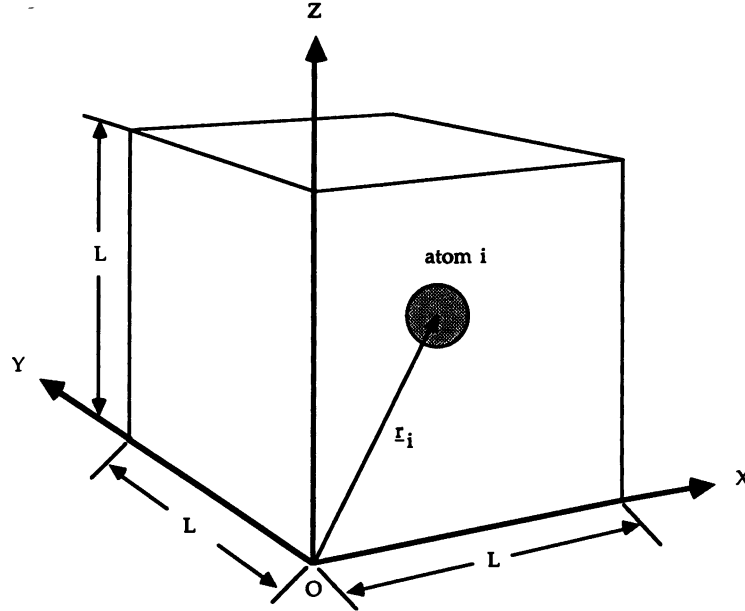
FIGURE 5.8 Space-fixed reference frame located with origin at one vertex of the cubic container having edges of length L. Sphere location vectors $\mathbf{r}_i$ are measured in this frame.

fore, we adjust the scaled initial velocities so that the total linear momentum is initially zero. The adjustment takes the form

$$v_{ix}^{*\,new}(0) = v_{ix}^{*}(0) - \frac{1}{N} \sum_j v_{jx}^{*}(0) \qquad (5.28)$$

with similar adjustments for $v_{iy}(0)$ and $v_{iz}(0)$.

Values for the initial accelerations $\mathbf{a}_i(0)$ are determined from the positions $\mathbf{r}_i(0)$ by computing the force on each atom, via (5.5), and applying Newton's second law. Thus, at this point we have values for $\mathbf{r}_i(0)$, $\mathbf{v}_i(0)$, and $\mathbf{a}_i(0)$. Besides these, the Gear algorithm uses the third, fourth, and fifth derivatives of the positions. To obtain initial values for these higher derivatives of $\mathbf{r}_i(0)$, we may evaluate derivatives of the force (5.5), but the calculations are tedious. Alternatively, initial values can be taken from the end of a previous simulation. A third scheme is to set the higher derivatives initially to zero,

$$\mathbf{r}_i^{(iii)}(0) = \mathbf{r}_i^{(iv)}(0) = \mathbf{r}_i^{(v)}(0) = 0 \qquad (5.29)$$

This means that for the first few time-steps of a run the fifth-order predictor is not being used; however, within about 50 time-steps, values of the higher
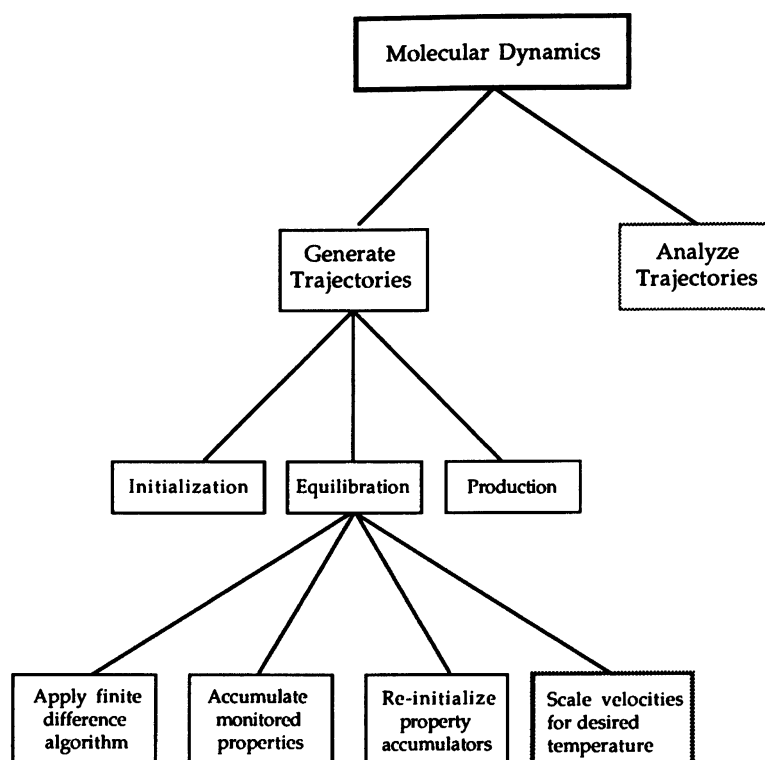
```
                    ┌──────────────────────┐
                    │  Molecular Dynamics  │
                    └──────────────────────┘
                       ╱              ╲
                      ╱                ╲
        ┌─────────────┐              ┌──────────────┐
        │  Generate   │              │   Analyze    │
        │ Trajectories│              │ Trajectories │
        └─────────────┘              └──────────────┘
          ╱     │     ╲
         ╱      │      ╲
┌──────────────┐ ┌─────────────┐ ┌────────────┐
│Initialization│ │Equilibration│ │ Production │
└──────────────┘ └─────────────┘ └────────────┘
              ╱   ╱    │    ╲     ╲
             ╱   ╱     │     ╲     ╲
┌──────────┐┌──────────┐┌───────────┐┌──────────────┐
│Apply finite││Accumulate││Re-initialize││Scale velocities│
│difference ││monitored ││property   ││for desired   │
│algorithm  ││properties││accumulators││temperature  │
└──────────┘└──────────┘└───────────┘└──────────────┘
```

FIGURE 5.9   Equilibration involves applying a finite-difference method to generate the trajectory and accumulating selected properties to monitor the system's relaxation from initial conditions. The velocity scaling is optional. At the end of equilibration, property accumulators are reset to zero so that properties are computed only along the equilibrium trajectory.

derivatives are accumulated and thereafter the full predictor–corrector algorithm is operational.

5.3   EQUILIBRATION

With initialization accomplished, the run itself can begin. Over the first few hundred time-steps the system relaxes from the arbitrarily assigned initial conditions and approaches equilibrium; this relaxation phase is called *equilibration*. As suggested in Figure 5.9, equilibration involves at least three, possibly four, distinct activities. The first is use of the finite-difference algorithm to generate the phase-space trajectory. The second is our monitoring of the trajectory by following selected properties. The third activity is optional: during equilibration we may continually scale the atomic velocities

to keep the system temperature close to a desired value. The last activity occurs at the end of equilibration when property accumulators are reinitialized to zero, so that properties are computed only over the equilibrium phase of the run. The duration of equilibration varies: it depends on how far removed the initial conditions are from the equilibrium state. The goal of equilibration is to ensure that values computed for equilibrium properties are not affected by how the simulation was started.

5.3.1 Approach to Equilibrium

During equilibration, running averages for most properties are not stable; rather, averages will be evolving toward their equilibrium values. However, because the system is isolated, the total energy should have the same value at each time-step even when the system is not yet at equilibrium. Conservation of total energy is sensitive to many small errors that can inadvertently creep into a simulation code; so, during equilibration without velocity scaling, energy conservation provides an important and direct indicator of errors in the program.

The evolution to equilibrium necessarily involves equilibration in both configuration space and momentum space, so we need quantities that monitor both. Just as for hard spheres, we use the positional order parameter λ to monitor the disintegration of the initial fcc lattice and use the instantaneous (kinetic) Boltzmann H-function to monitor the development of the equilibrium distribution of atomic velocities. Recall from Section 3.5.1 that the order parameter is defined by

$$\lambda = \tfrac{1}{3}\left[\lambda_x + \lambda_y + \lambda_z\right] \tag{3.41}$$

where

$$\lambda_x = \frac{1}{N}\sum_i^N \cos\left(\frac{4\pi x_i}{a}\right) \tag{3.42}$$

and a is the length of one edge of the fcc unit cell. Also in Section 3.5.2, we took one component of the H-function to be

$$H_x = \sum_{\Delta v_x} f(v_x)\ln f(v_x)\, \Delta v_x \tag{3.45}$$

where $f(v_x)$ is the distribution of the x-component of atomic velocities,

$$f(v_x)\, \Delta v_x = \frac{1}{N}\sum_i^N \delta(v_x - v_{xi})\, \Delta v_x \tag{3.44}$$

The behaviors of λ and H for soft spheres should be the same as for hard spheres: equilibration is not complete until λ is fluctuating about zero and

the H-function is near a value that is consistent with the Maxwell velocity distribution. Consult Section 3.5 for detailed discussions of these quantities.

5.3.2 Identification of Equilibrium

For an isolated system, a necessary and sufficient condition for identifying equilibrium is that the system entropy be a maximum. Unfortunately, entropy is not a measurable property and cannot be readily evaluated from the time average of some mechanical quantity (see Section 6.3). We are therefore left with the problem of identifying equilibrium by accumulating a number of necessary conditions and claiming that these are also sufficient.

Thermodynamic equilibrium encompasses thermal equilibrium, mechanical equilibrium, and chemical equilibrium. Thermal equilibrium means the absence of any driving forces for heat transfer, mechanical equilibrium means the absence of driving forces that would deform the size or shape of the system, and chemical equilibrium means the absence of driving forces that promote chemical reactions, phase transitions, and diffusional mass transfer. These driving forces must be absent not only across system boundaries but also across boundaries between any arbitrarily identified, macroscopic parts of the system.

Equilibrium eludes simple identification in molecular dynamics, first, because it is a macroscopic concept: it applies over a finite duration to a system of macroscopic size. Sampling the system at one instant is not sufficient to identify an equilibrium state. Second, equilibrium pertains to a finite duration that is important to the observer [11]. For example, the carbon-steel blade of a knife appears, over a few hours, to be in equilibrium with its surroundings; apparently, no driving forces are present to disturb its thermal, mechanical, or chemical equilibrium. However, after a few days of exposure to humid air, the blade has rusted. Is the knife in equilibrium with its surroundings or not? The answer depends on what time scale is of interest to the observer.

Here are some necessary conditions that an isolated system at equilibrium should satisfy:

1. The total number of molecules N and total energy E should be constants, independent of time. Since E is constant, fluctuations in the kinetic energy and potential energy must be equal in magnitude but out of phase with one another.

2. Each Cartesian component of the velocities should, on a time average, describe a Maxwell distribution (2.54),

$$f(v_x^*) \, \Delta v_x^* = \frac{1}{\sqrt{2\pi T^*}} \exp \frac{-v_x^{*2}}{2T^*} \, \Delta v_x^* \qquad (5.30)$$

where $f(v_x^*)\Delta v_x^*$ is the probability of finding a molecule whose x-component of velocity lies in $v_x^* \pm \frac{1}{2}\Delta v_x^*$. Recall, in our system of units (Table 5.2) the molecular mass is unity. As described in Section 3.5.2, the probability density $f(v_x^*)$ can be obtained from a molecular dynamics simulation by counting, at one instant, the number of molecules having x-velocities in $v_x^* \pm \frac{1}{2}\Delta v_x^*$, and averaging that number over time,

$$f(v_x^*)\Delta v_x^* = \frac{1}{N}\left\langle \sum_i^N \delta[v_x^* - v_{ix}^*]\Delta v_x^* \right\rangle \tag{5.31}$$

The y- and z-components of velocity should also have the distribution (5.30); moreover, the distribution should be independent of the orientation of the reference frame that defines the directions x, y, and z. A consequence of the Maxwell distribution of velocities is equipartition of kinetic energy (2.55). That is, each Cartesian component of the molecular velocities should, on a time average, give the same kinetic energy and hence the same temperature,

$$\frac{1}{N}\left\langle \sum_i v_{ix}^{*2} \right\rangle = \frac{1}{N}\left\langle \sum_i v_{iy}^{*2} \right\rangle = \frac{1}{N}\left\langle \sum_i v_{iz}^{*2} \right\rangle = T^* \tag{5.32}$$

Again, this equality should be satisfied regardless of the directions of x, y, and z.

3. Thermodynamic properties, such as the temperature, configurational internal energy, and pressure, should be fluctuating about stable average values. These averages should be independent of how the equilibrium state was attained. Thus, at a specified state condition, averages should be reproduced when a run is repeated from different assignments of initial positions and initial velocities. The magnitudes of the fluctuations depend on the system size, that is, on the number of atoms N; in particular, the fluctuations decrease as $N^{1/2}$. Thus, when we increase the number of atoms from 108 to 500, the magnitudes of fluctuations are roughly halved, as illustrated in Figure 5.10.

4. Property averages should be stable to small perturbations. If the state is disturbed, for example by momentarily adding then removing a small amount of heat, thermodynamic properties should recover their equilibrium values. Such small perturbations often can disrupt metastable states, which otherwise may exhibit some features of equilibrium.

To illustrate, Figure 5.11 shows the consequences of artifically increasing the instantaneous temperature in a simulation. The simulation used 108 atoms interacting via the Lennard-Jones shifted-force potential (5.12). At 5000 time-steps after equilibration, the velocities were scaled so as to increase the temperature by a factor of 1.5. This scaling was continued for 20 time-steps (0.17 psec), after which the velocities were rescaled for another 20 time-steps to regain the original value of the total energy ($E/N\varepsilon = -1.48$).
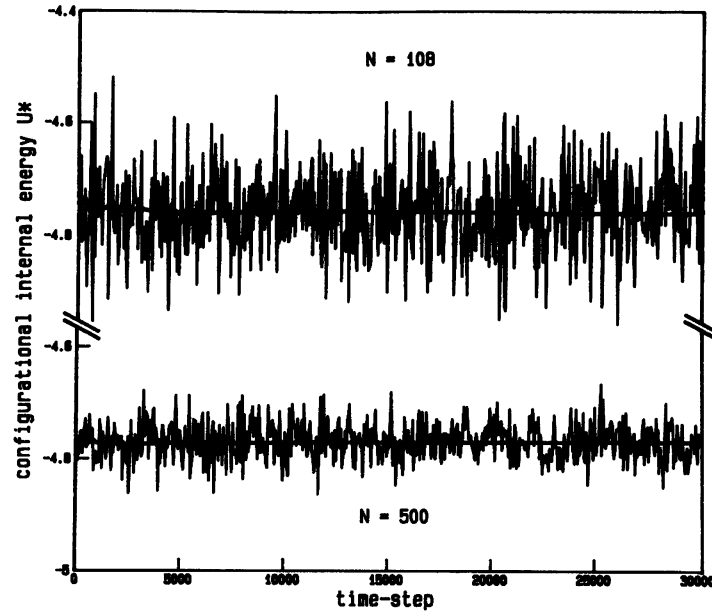
FIGURE 5.10 Magnitudes of fluctuations in instantaneous properties decrease as the number of particles is made larger. Here the configurational internal energy $\mathscr{U}^* = \mathscr{U}/N\varepsilon$ is shown from two simulations of the Lennard-Jones fluid, both at $\rho\sigma^3 = 0.7$ and $\langle kT/\varepsilon \rangle = 1.19$. The upper panel is for $N = 108$ atoms; the lower for $N = 500$ atoms. In each plot, the nearly horizontal line is the running average of the fluctuating values. Values are plotted here at intervals of 50 time-steps, where the time-step is $\Delta t^* = \Delta t/\sigma(m/\varepsilon)^{1/2} = 0.004$.

The figure indicates that both the instantaneous internal energy and the instantaneous pressure were unaffected by the perturbation.

5. If the system is divided into macroscopic parts, time averages for each property should be the same in each part. For example, imagine that we arbitrarily divide the system in half. When averaged over a finite duration, the number of molecules, temperature, total energy, and pressure in the two halves should each be the same.

None of these five conditions, individually or collectively, is sufficient to prove the existence of an equilibrium state. However, the more of these we can demonstrate, the stronger the case for claiming equilibrium, at least over the time-scale of the runs. These tests need not be applied to every run; rather, they are typically implemented in pilot runs before extensive production runs are done. However, they should be applied periodically during a series of production runs, especially after substantial changes have been made in state condition or potential model.
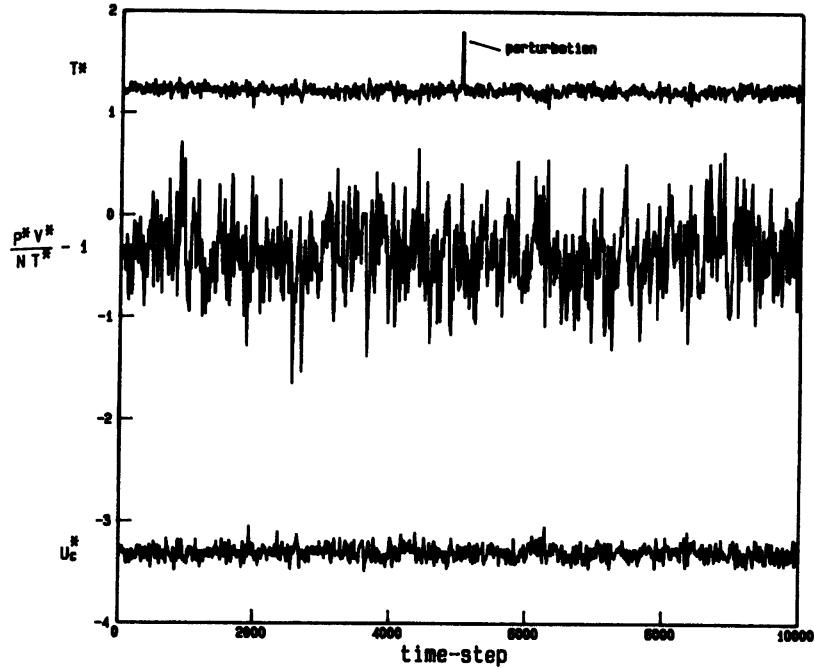
FIGURE 5.11 At equilibrium a system is stable to small perturbations. Here the instantaneous pressure and configurational internal energy are unaffected when, at time-step 5000, the temperature is momentarily increased by a factor of 1.5. These results are from a run of 108 atoms at $\rho\sigma^3 = 0.6$ and $\langle kT/\varepsilon \rangle = 1.22$. The potential used was the Lennard-Jones shifted-force model (5.12), with the shift at 2.5σ. The top line is temperature kT/ε, the middle line is pressure $P/\rho\langle T\rangle - 1$, and the bottom line is the potential energy $\mathscr{U}^* = \mathscr{U}/N\varepsilon$.

5.3.3 Fluid or Solid?

When simulations are performed at state points near the melting curve or whenever a simulation is started from a lattice structure, there is concern as to whether the system is solid or fluid throughout the simulation. We mention here three quantities that can be used to distinguish fluid from solid-like behavior. First is the positional order parameter, already discussed in Sections 5.3.1 and 3.5.1. A second indicator is the running mean-square displacement Δr^{*2}, defined by

$$\Delta r^{*2}(t) = \frac{1}{N} \sum_i \left[\mathbf{r}_i^*(t) - \mathbf{r}_i^*(0) \right]^2 \tag{5.33}$$

For a solid, $\Delta r^2(t)$ remains nearly constant, while for a fluid it increases almost linearly with time. (When $\Delta r^2(t)$ is averaged over many time origins,
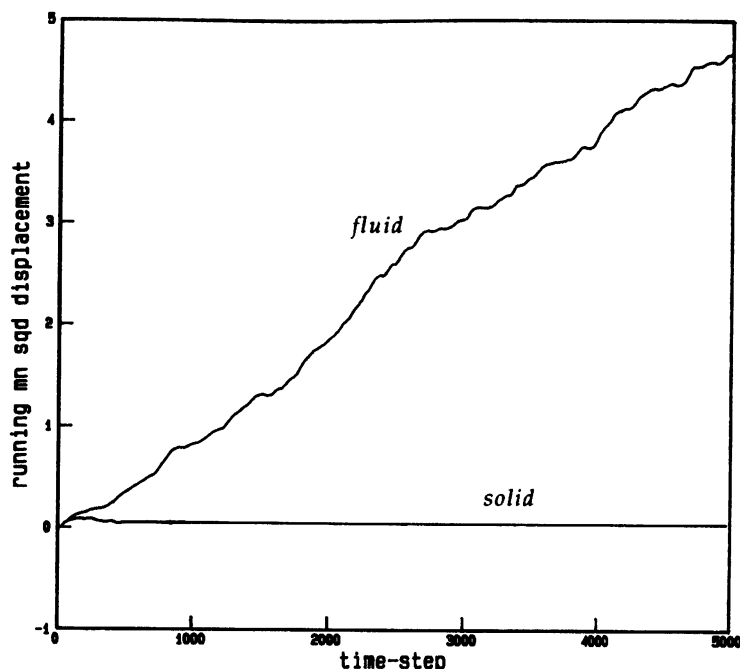
FIGURE 5.12 The running mean-square displacement (msd) can often be used to distinguish a fluid from a solid. Here the running msd, $\Delta r^{*2}(t)$ from (5.33), of Lennard-Jones atoms in a fluid state (upper line) is compared with that in a solid state (lower line). The simulations were each done using 256 atoms at $\rho\sigma^3 = 0.9$. The fluid state was at $\langle kT/\varepsilon \rangle = 1.087$, while the metastable solid was at $\langle kT/\varepsilon \rangle = 0.80$. See Figure 5.7 for the location of these states on the Lennard-Jones phase diagram.

it should be exactly linear; see Chapter 7.) In other words, a fluid has a self-diffusion coefficient that is several orders of magnitude larger than that for a solid. The fluid and solid behaviors of $\Delta r^2(t)$ are compared in Figure 5.12.

A third indicator is the radial distribution function $g(r)$. For partially crystallized fluids or partially melted solids, $g(r)$ may exhibit remnants of the underlying lattice structure; such remnants will be absent in the distribution functions of completely fluid phases. This use of the radial distribution function is discussed in Section 6.4.

5.4 PRODUCTION

Once equilibration is complete and we are satisfied that the system is at equilibrium, the production phase of the run can begin. Production introduces nothing new—the two basic activities used in equilibration are also

used in production: the code repeatedly applies the finite-difference algo-
rithm to follow the phase-space trajectory and it accumulates contributions to
properties. At intervals during production, we may save to disk or tape
certain quantities that can best be analyzed after the run is finished. Exam-
ples include quantities that lead to fluctuation properties (Chapter 6), to time
correlation functions (Chapter 7), and to estimates of statistical uncertainties
(Section 5.5).

The only remaining issue, then, is how long should the production run be?
Just as for hard spheres, the purpose of extending the length of a run is to
reduce statistical uncertainties (see Section 3.8.2). Recall that statistical
uncertainties decrease as the root of the run length. We determine the length
of run by first doing a short pilot run in which we compute properties and
their statistical uncertainties. We then identify the magnitude of statistical
uncertainty we are willing to tolerate, and finally, to obtain the needed
duration of the production run, we scale the pilot run length by the square of
the ratio of pilot uncertainty to desired uncertainty.

5.5 ASSESSING RELIABILITY OF RESULTS

At the end of a production run we are faced with the problem of assessing
the reliability of the results. The problem is the same as for hard spheres, so
if you managed to get this far without having read Section 3.8, you should go
back now and read it. This section, like Gaul, is divided into three parts:
Section 5.5.1 lists checks that can be used to test the code itself, Section 5.5.2
discusses statistical error, and Section 5.5.3 considers systematic error.

5.5.1 Checking Reliability of the Code

Here we list several tests that can be used to check a soft-sphere simulation
code. The list parallels that given in Section 3.8.1 for hard spheres, and as
there, the intention is merely to provide a listing for easy reference. The tests
cited here are only necessary conditions; they are not sufficient to prove that
a code is correct.

Equilibration

1. During equilibration, if no velocity scaling is being done, the total
   energy should be essentially constant.
2. By the end of equilibration:
   (a) The positional order parameter should be fluctuating about zero,
       with fluctuations having magnitudes $\leq \sqrt{N}/N$ (Section 3.5.1).
   (b) The H-function should be near a value consistent with the Maxwell
       velocity distribution (Sections 2.7.1 and 3.5.2).

Conservation Principles (Section 2.10)

3. The number of spheres in the primary cell should be constant with time.

4. Each Cartesian component of the total linear momentum should be zero.

5. The total energy should be constant with time.

Values of Properties

6. The kinetic energy should be equally partitioned among its three Cartesian components (Section 2.7.1).

7. Instantaneous property values should be stable, fluctuating about constant values.

8. Averages should be reproducible, within statistical uncertainties, when runs are repeated at the same state condition but from different initial conditions.

5.5.2 Statistical Error

Control of statistical error is linked to the duration of the production run (Section 5.4) and to the particular way we choose to sample the computed trajectory. Our first concern is to avoid serial correlations between instantaneous property values that are close to one another on the phase-space trajectory. In the discussion of statistical sampling in Section 2.8.4, we pointed out that a common strategy for avoiding serial correlations is to divide a computed phase-space trajectory into segments whose durations are longer than the relaxation time for the property of interest. For the Lennard-Jones fluid, we found (Figure 2.12) that relaxation times for simple properties, such as the pressure, are about one mean collision interval. Using time-steps of size $\Delta t^* = 0.004$, a collision interval is typically 40–50 time-steps; the exact duration depends on temperature and density. In Section 2.8.4 we suggested three sampling procedures that can help avoid serial correlations: stratified systematic sampling, stratified random sampling, and coarse graining. Any of the three can be used for soft spheres, and in fact, if we save to disk both instantaneous and running average values for properties, then we can apply both coarse graining and stratified systematic sampling and use the one that gives the smaller statistical uncertainty. Since we have discussed coarse graining in Section 3.8.2, we consider here stratified sampling.

In stratified systematic sampling for a property x, we simply draw instantaneous values $x(t)$ at a regular interval whose duration is greater than the relaxation time for serial correlations. Typically, every 50 time-steps is sufficient for simple thermodynamic properties. For example, from a production run of 50,000 time-steps, we would have a stratified systematic sample